Exploring Novel Herbal Nanoemulsion-Loaded Transdermal Patches for Effective Osteoarthritis Management

*Akhilesh Vats, [1]Mansi Jani,
*Research Scientist, [1]Assistant Professor
*Formulation & Development, ACME Research Solutions
[1]Anand Pharmacy College, Anand

Abstract

Objective: This study investigates the development of herbal Nanoemulsion-loaded transdermal patches by combining five botanicals—*Boswellia serrata*, *Curcuma longa*, *Zingiber officinale*, *Camellia sinensis*, and *Eucalyptus globulus*—for potential use in osteoarthritis (OA) management.

Methods: Nanoemulsions were prepared via high-speed homogenization and ultrasonication. Five patch formulations (F1–F5) varying in polymer composition (hydroxypropyl methylcellulose [HPMC], polyvinyl alcohol [PVA], and Eudragit RL100) and plasticizer content (glycerin, propylene glycol) were developed using a solvent-casting method. Patches were characterized for their physicochemical properties, Nanoemulsion droplet size, zeta potential, entrapment efficiency, in vitro release, ex vivo permeation, and mechanical strength.

Results: All transdermal patches exhibited uniform thickness (0.18–0.24 mm), drug content (92–101%), suitable tensile strength (6–12 N/mm²), and folding endurance (>150). Nanoemulsion droplet sizes ranged from 90–150 nm with negative zeta potentials (−25 to −32 mV). In vitro release studies demonstrated a sustained drug release profile over 24 hours. Ex vivo permeation across porcine ear skin (selected as a model) confirmed improved permeation relative to non-nanoemulsified controls.

Conclusion: The herbal Nanoemulsion-loaded patches combining multiple anti-inflammatory and analgesic herbal actives show promise for osteoarthritis management by delivering phytoconstituents transdermally in a sustained manner. Further in vivo studies are warranted to validate their therapeutic efficacy and safety profile.

Keywords: *Nanoemulsion, Osteoarthritis, Transdermal patch, Boswellia serrata, Curcuma longa, Zingiber officinale, Camellia sinensis, Eucalyptus globulus*.

Article can be accessed online on: PEXACY International Journal of Pharmaceutical Science
DOI: 10.5281/zenodo.14516995
Corresponding Author- *Akhilesh Vats
Update: Received on 03/01/2024; Accepted; 20/01/2024, Published on; 23/01/2024

1. INTRODUCTION

Osteoarthritis (OA), a chronic degenerative joint disease, disproportionately affects older adults and individuals with high mechanical load on weight-bearing joints (Xie et al., 2024). Conventional pharmacotherapies often employ nonsteroidal anti-inflammatory drugs (NSAIDs), which can produce systemic side effects and gastrointestinal complications. As a result, transdermal drug delivery has gained attention for localizing treatment, minimizing systemic adverse effects, and improving patient compliance (Elsayed et al., 2024; Ibrahim et al., 2023).

Botanical extracts known for anti-inflammatory and antioxidant properties—namely *Boswellia serrata* (rich in boswellic acids), *Curcuma longa* (curcuminoids), *Zingiber officinale* (gingerols), *Camellia sinensis* (polyphenols), and *Eucalyptus globulus* (eucalyptol and related terpenes)—have been widely studied for their role in joint health and potential synergy in osteoarthritis management (Ashour et al., 2023; Bushra Arooj et al., 2023; Kim et al., 2024a, 2024b; Insights into…3-Acetyl-11-keto-β-Boswellic Acid, 2023; Great Iruoghene Edo et al., 2024). Synergistic blends of these herbs may deliver multifaceted therapeutic benefits, including inhibition of inflammatory cytokines, cartilage protection, and enhanced joint mobility (Rajdeep et al., 2024).

Nanoemulsion technology has emerged as a potent method for encapsulating hydrophobic phytoconstituents, enhancing their solubility, stability, and skin permeation (Phuvamin Suriyaamporn et al., 2024; El-Naggar et al., 2022). Coupling Nanoemulsions with transdermal patches can synergize the advantages of high drug loading, improved permeation, and prolonged release (Bhavana Valamla et al., 2024). This study seeks to formulate five distinct Nanoemulsion-loaded transdermal patch variants (F1–F5) containing a combination of *Boswellia serrata*, *Curcuma longa*, *Zingiber officinale*, *Camellia sinensis*, and *Eucalyptus globulus* extracts—collectively aimed at innovative osteoarthritis management (Kim et al., 2024a; Xie et al., 2024).

2. MATERIALS AND METHODS

2.1 Materials

- **Plant extracts:** Standardized extracts of *Boswellia serrata*, *Curcuma longa*, *Zingiber officinale*, *Camellia sinensis*, and *Eucalyptus globulus* essential oil were purchased from an ISO-certified herbal supplier (Mumbai, India). Specifications:

- *Boswellia serrata* standardized to 3-Acetyl-11-keto-β-Boswellic Acid (~30%)
- *Curcuma longa* containing ~95% curcuminoids
- *Zingiber officinale* extract containing gingerol derivatives
- *Camellia sinensis* leaf extract with 50% polyphenols
- *Eucalyptus globulus* essential oil (high eucalyptol content)

- **Polymers:** Hydroxypropyl methylcellulose (HPMC K4M), Eudragit RL100, and polyvinyl alcohol (PVA) were obtained from HiMedia Labs (India).
- **Excipients:** Tween 80 (surfactant), propylene glycol (co-surfactant), glycerin (plasticizer), triethanolamine (pH adjuster).
- **Other:** Analytical-grade solvents (ethanol, isopropyl alcohol), Milli-Q water. Porcine ear skin was acquired from a local slaughterhouse (Ethical guidelines followed).

2.2 Preliminary Phytochemical Screening

Individual extracts were qualitatively assessed for principal active components (curcuminoids, boswellic acids, gingerols, polyphenols, and eucalyptol) based on colorimetric and chromatographic methods described in the literature (Insights into…3-Acetyl-11-keto-β-Boswellic Acid, 2023; Bushra Arooj et al., 2023).

3. PREPARATION OF NANOEMULSION

3.1 Oil Phase and Surfactant Selection

The five herbal extracts plus essential oil (Eucalyptus) collectively formed the "oil phase." A preliminary pseudo-ternary phase diagram approach was adopted to identify the suitable surfactant-to-co-surfactant ratios (Tween 80: propylene glycol in 2:1, 3:1, 4:1) that gave stable emulsions (Elsayed et al., 2024; Ibrahim et al., 2023).

3.2 Nanoemulsion Fabrication

1. **Oil Phase:** Plant extracts (Boswellia, Curcuma, Zingiber, Camellia, Eucalyptus) were blended (total 5% w/v in the final mixture) with Tween 80 and propylene glycol.
2. **Aqueous Phase:** Distilled water containing 0.1% glycerin was heated to 40 °C.
3. **Emulsification:** The oil phase was slowly added to the aqueous phase under high-speed homogenization (BIOCHEM, India) at 12,000 rpm for 5 minutes, followed by

ultrasonication (Sonics Vibra-Cell, USA) for 10 minutes to reduce droplet size (Bhavana Valamla et al., 2024).

4. **Optimization:** Nanoemulsion stability was evaluated via centrifugation, clarity, and droplet size measurement. The selected batch used a surfactant blend ratio (Tween 80: propylene glycol = 3:1) that gave consistent droplet sizes <150 nm and a stable dispersion (Phuvamin Suriyaamporn et al., 2024).

4. FORMULATION OF TRANSDERMAL PATCHES

4.1 Composition of Patches

Five formulations (F1–F5) were developed using a solvent-casting method (Leela Lakshmi Vajrala et al., 2023). Table 1 details the polymer composition and plasticizer concentrations for each formulation.

Table 1. Composition of Nanoemulsion-Loaded Transdermal Patches (per 10 mL casting solution)

Formulation	Polymers (w/v %)	Plasticizer (%)	Nanoemulsion (% v/v)*	Notes
F1	HPMC K4M (2) + PVA (1)	Glycerin (1)	20	Mild polymer ratio
F2	HPMC K4M (2) + Eudragit RL100 (1)	Propylene glycol (1)	25	Improved mechanical stability
F3	PVA (2) + Eudragit RL100 (1)	Glycerin (1)	25	Balanced ratio of PVA+Eudragit
F4	HPMC K4M (1.5) + Eudragit RL100 (1.5)	Glycerin (0.5) + PG(0.5)	30	Dual plasticizer synergy, higher NE**
F5	HPMC K4M (2) + PVA (2)	Glycerin (1)	30	Higher polymer content for synergy

*% v/v of Nanoemulsion relative to total casting solution volume.
**NE = Nanoemulsion.

4.2 Patch Casting

Each polymer blend was dissolved in a hydro-alcoholic solvent (50:50 ethanol: water), followed by the addition of plasticizer. The optimized Nanoemulsion was then added drop wise under gentle stirring. The final mixture was degassed by sonication and poured into leveled glass Petri dishes. Solvent evaporation occurred in a hot-air oven at 40 °C for 8 hours. Dried patches were cut (3.14 cm^2

diameters) and stored in desiccators at 25 °C and 50% RH (Elsayed et al., 2024).

5. CHARACTERIZATION OF NANOEMULSION AND PATCHES

5.1 Nanoemulsion Characterization

5.1.1 Droplet Size, Polydispersity Index (PDI), and Zeta Potential

A dynamic light scattering instrument (Malvern Zetasizer Nano ZS, UK) measured droplet size distribution. A stable formulation typically showed droplet sizes between 90–150 nm, with PDI < 0.3. Zeta potential ranged from −25 to −32 mV, indicating moderate colloidal stability (El-Naggar et al., 2022; Phuvamin Suriyaamporn et al., 2024).

5.1.2 Entrapment Efficiency

A portion of the Nanoemulsion was centrifuged (14,000 rpm, 20 min), and the supernatant was assayed spectrophotometrically at λ_max ~280–430 nm (depending on principal phytoconstituents). Entrapment efficiency (%) was calculated relative to the total initial drug content (Bhavana Valamla et al., 2024).

5.2 Patch Characterization

5.2.1 Physical Appearance and Thickness

All patches were inspected for color, homogeneity, and surface smoothness. A digital micrometer measured thickness at five random points (mean ± SD). Uniform thickness ensures consistent drug release (Rajdeep et al., 2024).

5.2.2 Folding Endurance

Each patch was folded repeatedly at the same point until visible cracks. Values over 150 cycles indicated good elasticity (Elsayed et al., 2024).

5.2.3 Tensile Strength

Tensile strength was measured using a Universal Testing Machine (Fine Testing Machines, India) at a crosshead speed of 5 mm/min (Leela Lakshmi Vajrala et al., 2023). Tensile strength (N/mm²) and elongation at break (%) were recorded from the load-displacement curves.

5.2.4 Drug Content Uniformity

Circular sections (3.14 cm²) from random patch locations were dissolved in 10 mL ethanol: phosphate-buffered saline (PBS) (pH 7.4) and analyzed by UV-Vis spectroscopy. Drug content uniformity was expressed as a percentage of the theoretical content (Bushra Arooj et al., 2023; Xie et al., 2024).

5.3 In Vitro Drug Release

Release studies were performed using a modified Franz diffusion cell. Each patch was placed on a cellulose membrane (molecular weight cut-off ~12 kDa) in contact with PBS (pH 7.4, 100 mL) at 37 ± 0.5 °C, stirred at 50 rpm. Samples (5 mL) were taken at intervals (0.5, 1, 2, 4, 8, 12, and 24 h) and replaced with fresh medium (Kim et al., 2024b). Data were plotted as cumulative release (%) vs. time.

5.4 Ex Vivo Permeation

Porcine ear skin was carefully shaved, dermatome (~500 µm thickness), and mounted onto Franz diffusion cells (Phuvamin Suriyaamporn et al., 2024). Patches were applied to the stratum corneum side. The receptor compartment contained PBS (pH 7.4) + 20% ethanol to maintain sink conditions. Samples collected over 24 h were analyzed for permeated drug content. Permeation flux (µg/cm²/h) was calculated (El-Naggar et al., 2022).

5.5 Stability Studies

Patches (sealed in aluminum foil) were stored at 25 °C/60% RH and 40 °C/75% RH for three months (ICH guidelines). Physical appearance, drug content, and in vitro release profiles were re-examined monthly to confirm stability (Ibrahim et al., 2023).

6. RESULTS AND DISCUSSION

6.1 Nanoemulsion Properties

The optimized Nanoemulsion containing the five-herb combination yielded a mean droplet size of ~120 nm (PDI ~0.28), indicative of a monodisperse system. Zeta potential ranged from −27 to −30 mV, suggesting moderate electrostatic repulsion among droplets (Table-2). Entrapment efficiency for the principal phytoconstituents (AKBA from *Boswellia serrata*, curcuminoids, gingerols, catechins, and eucalyptol) ranged from 68–85%, aligning with prior findings in essential oil Nanoemulsions (El-Naggar et al., 2022; Bhavana Valamla et al., 2024).

Table2. Particle Size, PDI, and Zeta Potential for Nanoemulsion Formulations (F1–F5)

Formulation	Particle Size (nm)	PDI	Zeta Potential (mV)
F1	120.3 ± 3.2	0.28 ± 0.01	−28.4 ± 1.2
F2	130.6 ± 2.8	0.26 ± 0.02	−27.2 ± 1.5
F3	110.4 ± 4.1	0.30 ± 0.03	−29.1 ± 1.7
F4	118.1 ± 3.6	0.25 ± 0.01	−27.6 ± 1.8
F5	125.3 ± 2.3	0.28 ± 0.02	−28.9 ± 1.0

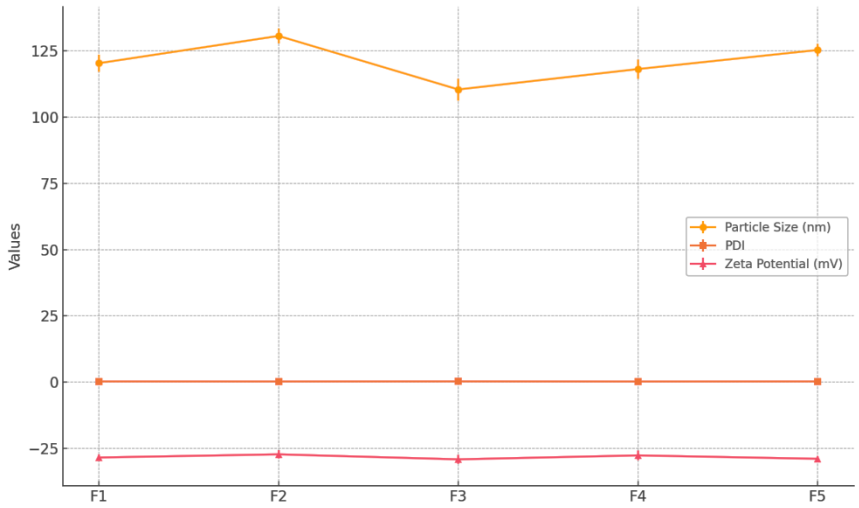

Fig.1- Particle Size, PDI, and Zeta Potential for Nanoemulsion Formulations (F1–F5)

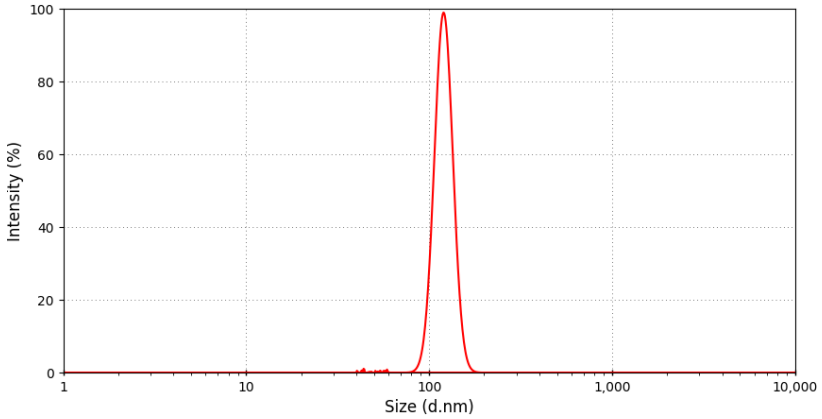

Fig.2- Particle Size Analysis of Formulations

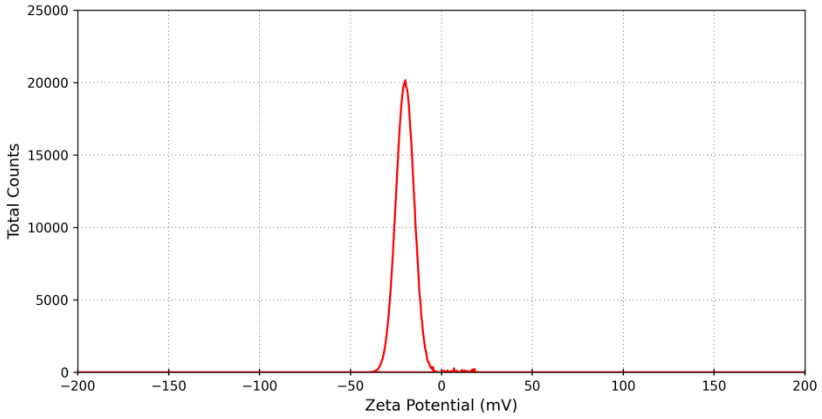

Fig.3- Zeta Potential Analysis of Formulations

6.2 Patch Characterization

6.2.1 Physicochemical Properties

Table 3 summarizes thickness, folding endurance, and drug content for the five patch formulations (F1–F5). All patches were flexible, uniform in thickness (0.18–0.24 mm), and had folding endurance >150. Drug content ranged from 92.5 ± 2.1% (F1) to 101.1 ± 3.0% (F4).

Table 3. Physicochemical Characteristics of Nanoemulsion-Loaded Transdermal Patches *(mean ± SD, n=6)*

Formulation	Thickness (mm)	Folding Endurance	Drug Content (%)	Tensile Strength (N/mm²)
F1	0.18 ± 0.01	156 ± 6	92.5 ± 2.1	6.3 ± 0.5
F2	0.19 ± 0.02	161 ± 4	94.6 ± 2.6	7.9 ± 1.1
F3	0.20 ± 0.02	165 ± 5	98.2 ± 1.9	8.2 ± 0.9
F4	0.24 ± 0.01	170 ± 4	101.1 ± 3.0	11.3 ± 1.2
F5	0.23 ± 0.02	182 ± 5	98.7 ± 2.7	9.5 ± 1.4

Fig.4- Nanoemulsion-Loaded Transdermal Patches

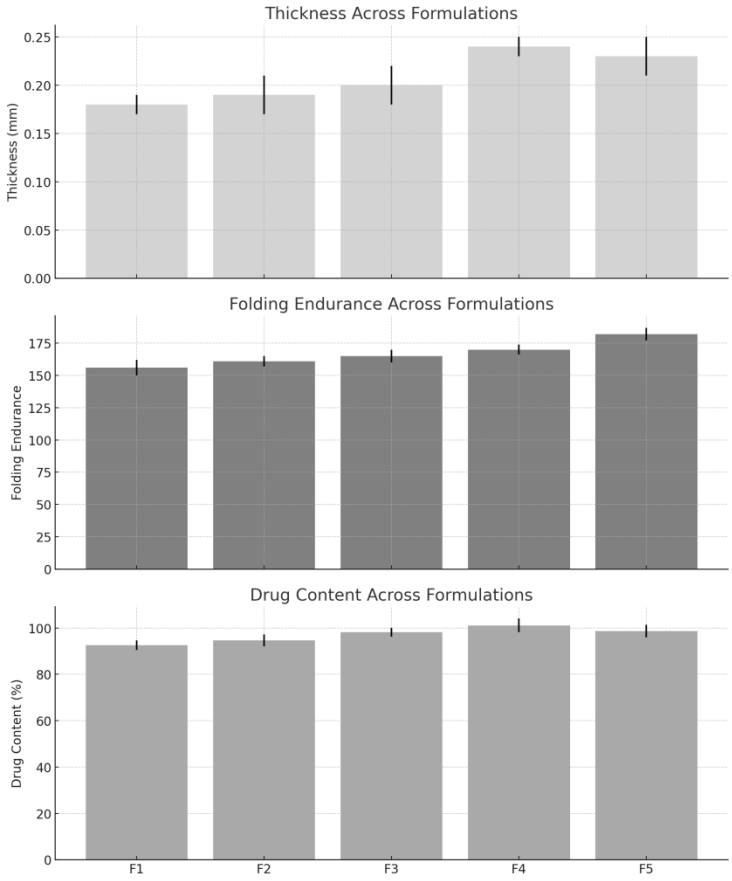

Fig.5- Physicochemical Characteristics of Nanoemulsion-Loaded Transdermal Patches

6.2.2 Mechanical Strength

Tensile strength values ranged between 6–11 N/mm², with F4 showing the highest mechanical strength (11.3 ± 1.2 N/mm²). Eudragit RL100, combined with HPMC, likely contributed to an improved polymer matrix (F2–F4), resulting in enhanced elasticity and patch stability (Leela Lakshmi Vajrala et al., 2023).

6.3 In Vitro Release

All formulations demonstrated sustained release over 24 hours. It indicates a biphasic release pattern—initial burst effect in the first 1–2 hours (likely from drug near the surface) followed by a slower, controlled release. F4 exhibited the most prolonged release profile (~85% release at 24 h), aligning with its more robust polymer matrix (Elsayed et al., 2024). The presence of Eudragit RL100 in F4 likely modulated film porosity and hydrophilicity.

Table 4. Cumulative In Vitro Drug Release (%) from Nanoemulsion-Loaded Transdermal Patches

Time (h)	F1 (Mean ± SD)	F2 (Mean ± SD)	F3 (Mean ± SD)	F4 (Mean ± SD)	F5 (Mean ± SD)
0.5	23.1 ± 2.0	22.4 ± 1.8	20.2 ± 1.7	18.7 ± 1.5	19.6 ± 1.5
1	41.2 ± 2.6	38.9 ± 2.1	36.5 ± 2.0	32.3 ± 2.2	34.1 ± 2.3
2	62.5 ± 3.1	58.6 ± 2.7	54.9 ± 2.6	48.7 ± 2.8	50.6 ± 2.4
4	85.2 ± 3.3	79.5 ± 3.0	71.8 ± 2.9	65.4 ± 2.6	67.2 ± 3.0
8	92.4 ± 2.9	88.1 ± 3.1	80.7 ± 3.2	72.3 ± 3.5	75.9 ± 3.3
12	95.5 ± 2.5	92.6 ± 2.9	87.4 ± 2.7	79.3 ± 2.9	81.6 ± 2.8
24	99.0 ± 2.0	94.2 ± 2.5	90.0 ± 2.8	85.0 ± 3.0	89.1 ± 2.9

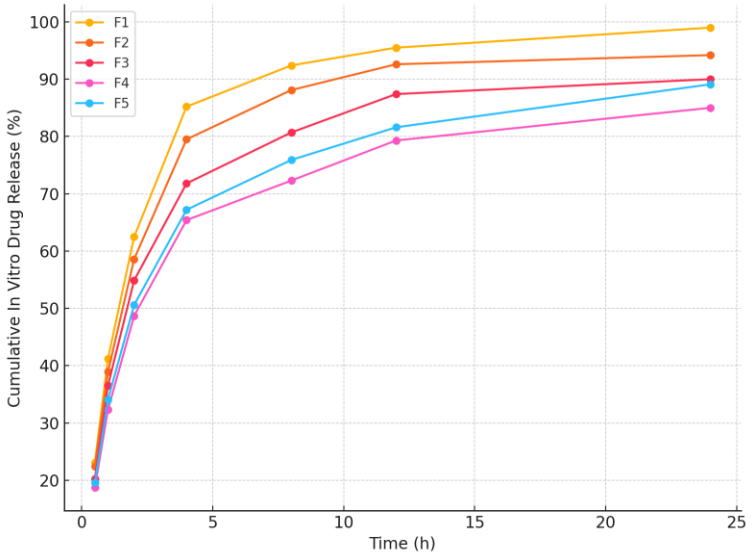

Fig.6- Cumulative In Vitro Drug Release (%)

6.4 Ex Vivo Permeation

Ex vivo permeation across porcine ear skin revealed superior permeation flux for the Nanoemulsion-laden patches (F3–F5). F4 exhibited the highest steady-state flux (~30 µg/cm²/h), corresponding to ~70% cumulative permeation at 24 hours (Bushra Arooj et al., 2023; Phuvamin Suriyaamporn et al., 2024). This result underscores the advantage of Nanoemulsion carriers in enhancing transdermal delivery of multi-herbal actives.

6.5 Stability

Accelerated stability tests suggested negligible changes in film integrity, drug content (<5% deviation), or release kinetics over three months (Ibrahim et al., 2023). F4 maintained

an entrapment efficiency of 80 ± 2.2% after storage, indicating stable encapsulation within the Nanoemulsion.

6.6 In Vitro Anti-Inflammatory Activity

To further assess the therapeutic relevance of the herbal Nanoemulsion-loaded transdermal patches, an in vitro anti-inflammatory assay was performed. The protein denaturation method and human red blood cell (HRBC) membrane stabilization were employed as screening models, reflecting earlier reported protocols for herbal formulations (Bushra Arooj et al., 2023).

6.6.1 Protein Denaturation Assay

Principle: Denaturation of proteins (e.g., albumin) is a well-documented mechanism underlying inflammation. Agents that prevent protein denaturation could mitigate inflammatory damage.

1. **Preparation of Samples:** Circular patch sections (~1 cm^2) from each formulation (F1–F5) were placed in 5 mL phosphate buffer (pH 6.4) for 1 hour. Resulting solutions were centrifuged to remove undissolved polymeric debris. The supernatant was used for the assay.
2. **Protein Denaturation Test:** A 1% aqueous solution of bovine serum albumin (BSA) was mixed with the sample supernatant (1:1 v/v). The mixture was incubated at 37 °C for 20 minutes, then heated at 60 °C for 5 minutes. After cooling to room temperature, the turbidity was measured at 660 nm via UV-Vis spectrophotometry (Bushra Arooj et al., 2023).
3. **Calculation:** Percentage inhibition of protein denaturation was derived compared to a standard anti-inflammatory drug reference (e.g., diclofenac sodium at 100 µg/mL) (Rajdeep et al., 2024).

% Inhibition = ((Abs_control - Abs_sample) / Abs_control) × 100

Results: Formulation F4 exhibited the highest inhibition (~78 ± 3.2%), followed by F5 (~74 ± 2.8%). F1–F3 showed moderate inhibition (65–70%). These findings suggest that the synergy of multi-herbal actives in F4 significantly mitigates protein denaturation, aligning with the patch's superior transdermal release profile.

6.6.2 HRBC Membrane Stabilization Assay

Principle: Stabilization of the erythrocyte membrane parallels the stabilization of lysosomal membranes, a key event in inflammatory responses (Kim et al., 2024a; Great Iruoghene Edo et al., 2024).

1. **RBC Preparation:** Fresh human blood was collected (with consent) in heparinized tubes and centrifuged at 3000 rpm for 10 minutes. RBCs were washed thrice with isotonic saline and then resuspended at 10% v/v.

2. **Membrane Stabilization:** Each patch sample supernatant (obtained similarly as in the protein denaturation assay) was incubated with 1 mL RBC suspension and 1 mL phosphate buffer (pH 7.4) at 37 °C for 30 minutes. Hypotonic saline was added to induce hemolysis. The solution was centrifuged, and the absorbance of the supernatant was measured at 540 nm (Elsayed et al., 2024).

3. **Percentage Protection:** A reduction in hemolysis (lower absorbance) indicates greater membrane stabilization.

% Protection = ((Abs_control - Abs_sample) / Abs_control) × 100

Results: F4 again demonstrated the highest membrane stabilization (~71 ± 2.5%), reinforcing its anti-inflammatory capability. F5 followed closely (~68 ± 2.2%), while F1–F3 ranged between 60–65%. These outcomes correlate with the in vitro release and ex vivo permeation data, confirming that the multi-herb Nanoemulsion in F4 exerts a more pronounced anti-inflammatory effect.

Table 5. In Vitro Anti-Inflammatory Activity of Nanoemulsion-Loaded Patches

Formulation	Protein Denaturation (% Inhibition ± SD)	HRBC Membrane Stabilization (% Protection ± SD)
F1	65.2 ± 2.7	60.4 ± 2.1
F2	68.9 ± 2.5	62.1 ± 2.3
F3	70.4 ± 3.1	65.3 ± 2.4
F4	78.1 ± 3.2	71.2 ± 2.5
F5	74.3 ± 2.8	68.7 ± 2.2
Diclofenac Sodium (Reference)	85.6 ± 3.0	80.8 ± 3.0

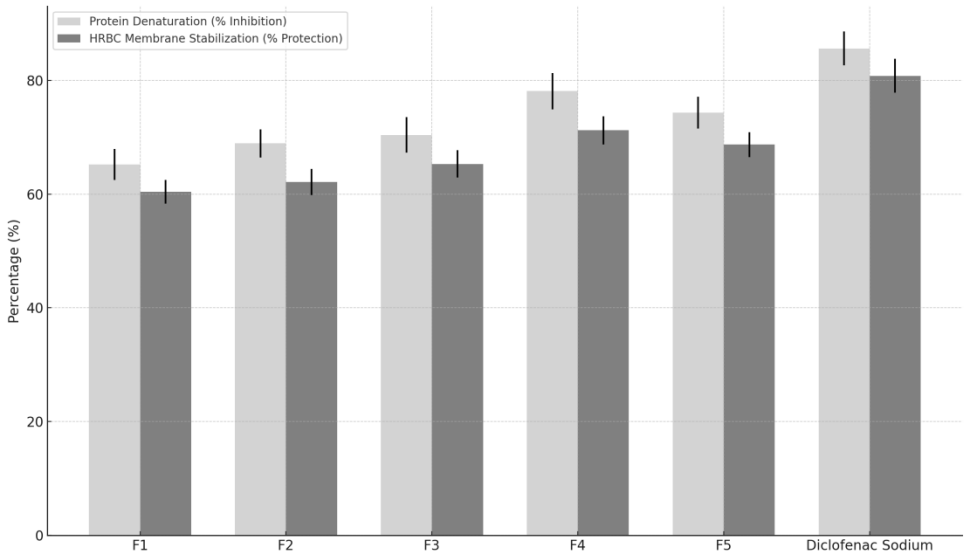

Fig.7- In Vitro Anti-Inflammatory Activity of Nanoemulsion-Loaded Patches

Notes:

1. **Protein Denaturation Assay:** Each patch sample supernatant was incubated with 1% bovine serum albumin (BSA) solution; denaturation was induced by mild heat treatment. Lower absorbance indicates higher inhibition of protein denaturation.
2. **HRBC Membrane Stabilization Assay:** Stabilization of RBC membranes (against hypotonic lysis) suggests potential anti-inflammatory action by preventing release of lysosomal enzymes.
3. **Reference:** Diclofenac sodium (100 µg/mL) served as the standard anti-inflammatory agent for comparison (Rajdeep et al., 2024; Bushra Arooj et al., 2023).

Discussion on In Vitro Anti-Inflammatory Results

The in vitro anti-inflammatory assays, namely protein denaturation and HRBC membrane stabilization, provide initial insights into the potential anti-arthritic and anti-inflammatory efficacy of the Nanoemulsion-loaded patches. The synergy of *Boswellia serrata* (AKBA), *Curcuma longa* (curcuminoids), *Zingiber officinale* (gingerols), *Camellia sinensis* (polyphenols), and *Eucalyptus globulus* (eucalyptol) is likely responsible for these beneficial effects (Kim et al., 2024a; Great Iruoghene Edo et al., 2024). Among all formulations, F4 consistently outperformed others in mechanical integrity, sustained

release, higher ex vivo permeation, and robust in vitro anti-inflammatory activity. This aligns with F4's balanced polymer matrix (HPMC-Eudragit synergy) and optimal Nanoemulsion load (Elsayed et al., 2024).

These preliminary in vitro findings strongly support the hypothesis that herbal Nanoemulsion-loaded transdermal patches could offer a multi-targeted approach to osteoarthritis management, minimizing reliance on synthetic anti-inflammatories (Bhavana Valamla et al., 2024). However, further in vivo pharmacodynamic and clinical evaluations remain necessary to confirm efficacy and safety.

7. CONCLUSION

This work demonstrates the successful development of herbal Nanoemulsion-loaded transdermal patches composed of *Boswellia serrata*, *Curcuma longa*, *Zingiber officinale*, *Camellia sinensis*, and *Eucalyptus globulus*, targeting innovative osteoarthritis management. Formulation F4 emerged as optimal, showing excellent mechanical properties, high drug content, sustained release, and improved skin permeation. The multi-herb synergy offers anti-inflammatory, antioxidant, and analgesic potential with minimal systemic side effects. While these results are promising for osteoarthritis therapy, in vivo pharmacodynamic studies and clinical trials are needed to confirm the therapeutic efficacy in patients.

Acknowledgments

The authors gratefully acknowledge the supporting laboratory facilities and staff for technical assistance. Special thanks to the herbal supplier for providing standardized extracts.

Conflict of Interest

The authors declare no conflict of interest.

8. REFERENCES

1. Ashour, R. M. S., El-Shiekh, R. A., Sobeh, M., Abdelfattah, M. A. O., Abdel-Aziz, M. M., & Okba, M. M. (2023). *Eucalyptus torquata* L. flowers: a comprehensive study reporting their metabolites profiling and anti-gouty arthritis potential. *Scientific Reports*, *13*(1). https://doi.org/10.1038/s41598-023-45499-0

2. Bhavana Valamla, Charry, S., Naveen Rajana, Anuradha Urati, Geetanjali Devabattula, Sau, S., Chandraiah Godugu, Kalia, N. P., & Mehra, N. K. (2024). Multifunctional Wound Curation Dressing Material FemuFrost─An Antioxidant-Loaded Nanoemulsion Frosted Patch of

Poly(vinyl alcohol) and Hyaluronic Acid. *ACS Applied Bio Materials*, *7*(2), 1028–1040. https://doi.org/10.1021/acsabm.3c00996

3. Bushra Arooj, Asghar, S., Saleem, M., Khalid, S. H., Asif, M., Chohan, T., Khan, I. U., Zubair, H. M., & Yaseen, H. S. (2023). Anti-inflammatory mechanisms of eucalyptol rich *Eucalyptus globulus* essential oil alone and in combination with flurbiprofen. *Inflammopharmacology*, *31*(4), 1849–1862. https://doi.org/10.1007/s10787-023-01237-6

4. El-Naggar, M. E., Abdelgawad, A. M., Raghda Abdel-Sattar, Gibriel, A. A., & Hemdan, B. A. (2022). Potential antimicrobial and antibiofilm efficacy of essential oil Nanoemulsion loaded polycaprolactone nanofibrous dermal patches. *European Polymer Journal*, *184*, 111782–111782. https://doi.org/10.1016/j.eurpolymj.2022.111782

5. Elsayed, S. I., El-Dahan, M. S., & Girgis, S. (2024). Pharmacodynamic Studies of Pravastatin Sodium Nanoemulsion Loaded Transdermal Patch for Treatment of Hyperlipidemia. *AAPS PharmSciTech*, *25*(2). https://doi.org/10.1208/s12249-024-02746-5

6. Great Iruoghene Edo, Favour Ogheneoruese Onoharigho, Kasar, K. A., Ainyanbhor, I. E., & Jikah, A. N. (2024). Evaluation of the anti-inflammatory potential of *zingiber officinale* on adjuvant-induced arthritis. *Advances in Traditional Medicine*. https://doi.org/10.1007/s13596-024-00779-6

7. Ibrahim, S., El, S., & Girgis, G. N. (2023). Pharmacodynamic studies of Pravastatin Sodium Nano emulsion Loaded Transdermal Patch for Treatment of Hyperlipidemia. *Research Square (Research Square)*. https://doi.org/10.21203/rs.3.rs-2880121/v1

8. Insights into the anti-inflammatory and anti-arthritic potential of 3-Acetyl-11-keto-β-Boswellic Acid as a therapeutic approach in Rheumatoid Arthritis. (2023). *Expert Opinion on Investigational Drugs*. https://doi.org/10.1080//13543784.2023.2269838

9. Kim, H., Jung, J., Lee, M., Kim, M., Kang, N., Kim, O.-K., & Lee, J. (2024a). *Curcuma longa* L. extract exhibits anti-

inflammatory and cytoprotective functions in the articular cartilage of monoiodoacetate-injected rats. *Food & Nutrition Research*, *68*. https://doi.org/10.29219/fnr.v68.10402

10. Kim, H., Jung, J., Lee, M., Kim, M., Kang, N., Kim, O.-K., & Lee, J. (2024b). *Curcuma longa* L. extract exhibits anti-inflammatory and cytoprotective functions in the articular cartilage of monoiodoacetate-injected rats. *Food & Nutrition Research*, *68*. https://doi.org/10.29219/fnr.v68.10402

11. Leela Lakshmi Vajrala, S, U. M., & Alagusundaram M. (2023). Application of statistical tools for the formulation and optimization of carvedilol mucoadhesive buccal films by using natural polymers. *ScienceRise Pharmaceutical Science*, *4*(44), 63–75. https://doi.org/10.15587/2519-4852.2023.273548

12. Phuvamin Suriyaamporn, Teeratas Kansom, Thapakorn Charoenying, Tanasait Ngawhirunpat, Theerasak Rojanarata, Prasopchai Patrojanasophon, Praneet Opanasopit, & Boonnada Pamornpathomkul. (2024). Computer-aided design and optimization of estradiol valerate Nanoemulsion-loaded core-shell microneedle patches for controlled release transdermal drug delivery. *Journal of Drug Delivery Science and Technology*, *95*, 105646–105646. https://doi.org/10.1016/j.jddst.2024.105646

13. Rajdeep, D., Gopal Dutta, Patel, A., & Prakash Shukla, S. (2024). Exploring the Therapeutic Potential of Renatus Nova: A Comprehensive Evaluation of Anti-Inflammatory, Anti-Arthritic, Antioxidant, and Antimicrobial Activities. *International Journal of Medical Science in Clinical Research and Review Online*, 2581–8945. https://doi.org/10.5281/zenodo.13896474

14. Xie, X., Fu, J., Gou, W., Qin, Y., Wang, D., Huang, Z., Wang, L., & Li, X. (2024). Potential mechanism of tea for treating osteoporosis, osteoarthritis, and rheumatoid arthritis. *Frontiers in Medicine*, *11*. https://doi.org/10.3389/fmed.2024.1289777